

MODELLING COMPRESSIBLE AND UNDER-EXPANDED JETS WITH SECOND-MOMENT CLOSURE

P. R. Ess* and M. A. Leschziner

Department of Aeronautics,
Imperial College London,
Prince Consort Road,
London, SW7 2AZ, UK
peter.ess@dlr.de and mike.leschziner@imperial.ac.uk

ABSTRACT

Compressible and under-expanded jets with a nozzle-pressure ratio (NPR) up to 3 are computed with a two-component-limit second-moment closure and modifications to account for effects of compressibility on turbulence. The results are compared to experimental data from LDA measurements. Good agreement is observed for the baseline turbulence model beyond the potential core. In contrast, for the range of NPRs studied, model modifications, specifically designed to replicate the effects of compressibility in shear layers, tend to worsen the results for the jet flows. Although the model predicts well the shock-cell structure in the potential core at high NPRs, the core tends to be too long, and a much higher level of discharge turbulence than that measured is required to procure reasonable agreement. Differences in the core in respect of turbulence intensity are argued to partially reflect experimental limitations.

INTRODUCTION

Under-expanded jets behind aircraft afterbodies are of principal interest in the context of wave drag, noise pollution and infrared observability. While afterbody drag has been the subject of previous research by the present group (Leschziner et al., 2001), the current work specifically seeks to improve the capability of modelling and predicting the fundamental interactions among turbulence, shear and compressibility effects in under-expanded jets.

Previous numerical work with statistical closures applied to under-expanded jets was undertaken by Dash et al. (1985) and Seiner et al. (1985), using a specialised code to study shock-noise features and employing a two-equation compressibility-corrected turbulence model. A further study by Pao and Abdol-Hamid (1996), again within the framework of two-equation turbulence models, focused on aerodynamic aspects of the jet, including mode-switching of non-axisymmetric jets. However, none of these studies deal in any detail with the modelling of effects of compressibility on turbulence.

Over the past decade, the application of large-eddy simulation (LES) to compressible flows has increased steadily. Until about 2003, attention was limited to fully expanded conditions - for example, Anderson (2003). However, more recently, several studies have been reported on shock-containing jets, mostly in relation to noise generation - for example, Viswanathan et al. (2005), Berland et al. (2006) and Bodony et al. (2006).

While LES undoubtedly offers many advantages over statistical modelling - notably, structural information needed

for direct noise prediction - it remains virtually untenable, on cost grounds, in practical circumstances in which the jet is part of a more complex scenario that might involve shock-boundary-layer interaction on complex aircraft bodies at high Reynolds numbers. In such circumstances, statistical modelling is the only practical predictive framework.

Past research on shock-induced boundary-layer separation (Batten et al., 1999, Leschziner et al., 2001) may be claimed to demonstrate the advantages that can be derived from second-moment closure, relative to two-equation modelling. These advantages arise from the fact that the former framework accounts for anisotropy and the turbulence production which depends strongly on it. Leschziner et al. (2001) show, in particular, that the two-component-limit (TCL) model of Craft and Launder (1998), modified by Batten et al. (1999) for shock-containing flows, performs well in afterbody flows. It is this model that is also the focus of the present paper.

Specifically in relation to effects of compressibility in free shear layers, the simulations of Vreman et al. (1996) and Pantano and Sarkar (2002) offer information that is potentially useful for improving second-moment closure. These studies indicate that compressibility affects turbulence primarily through an alteration of the pressure-strain-interaction process within the balance equations that govern the Reynolds stresses. This is in contrast to previous assumptions on, and related modelling efforts targeting, explicit dilatational dissipation and pressure-velocity fragments. Among other issues, the present work examines the usefulness of information derived from the simulation in modelling of the pressure-strain tensor with the cubic pressure-strain approximation that is part of the above-mentioned two-component limit second-moment closure.

The implicit flow solver developed by Batten et al. (1997) provides the baseline numerical method employed for this study. Based on the model proposed by Pantano and Sarkar (2002) for the attenuation of the pressure-strain process in terms of convective Mach number of a shear layer, a suitable extension is sought for jets, that represents the effects of compressibility correctly in terms of the gradient Mach number, for both compressible shear layer and jet flows. Studies both without and with compressibility corrections have been performed, and the target is to optimise an approach that sensitises appropriately the pressure-strain process itself (rather than additional correction terms) to compressibility, expressed by the gradient Mach number.

The work on turbulence modelling is complemented by experimental studies of fully- and under-expanded jets (Feng and McQuirk, 2005), providing LDA data of velocities and Reynolds stresses for model validation. Round jets of air in a range of nozzle-pressure ratios (NPR) from 1.45 to 3.00

*present address: DLR-VT, Pfaffenwaldring 38-40, 70569 Stuttgart, Germany

were studied, with the critical NPR being 1.89. A convergent nozzle with diameter of $D = 0.048m$ was used in the experiments.

In the following sections, the computational approach is introduced and the modelling of compressibility in turbulent shear flows is discussed, with particular attention to compressible mixing layers. The main section of the article presents the results for the fully- and under-expanded jets, a detailed comparison with measured data and a discussion of the key findings.

COMPUTATIONAL APPROACH

The computational scheme is based on the HLLC approximate Riemann solver with van-Leer's TVD flux limiter, combined with implicit time-marching, as described by Batten et al. (1997). This allows very high values for the CFL number, restricted to 25 in the present application. The algorithm is fully three-dimensional, but was used here to compute an azimuthal segment, subject to homogeneity conditions at the azimuthal planes.

Turbulence modelling aside, under-expanded jets pose considerable numerical problems associated with the need to resolve the correct sequence of decaying shock-cell train that arises from the interaction of oblique shocks with the shear layer. This requires refined numerical techniques, coupled with very close attention to the computational grid. The numerical challenges are especially severe when modelling is at non-linear second-moment level, as is the case herein. The computational domain expanded with the jet, covering 50 nozzle diameters in streamwise direction and 10 – 25 diameters in the radial direction. The mesh density was varied between 443×86 and 817×113 lines. Careful attention was paid to the cell aspect ratio and the level of grid expansion, not allowed to exceed 1.05. Without this attention, the shock train, shown in Fig. 1 for NPRs 2.06, 2.32 and 3.00, cannot be captured with credible realism.

MODELLING EFFECTS OF COMPRESSIBILITY

Compressibility is known to provoke a steep decline in the spreading rate of supersonic free shear layers with increasing convective Mach number $Ma_c = \Delta U / (2a)$ (Papamoshou and Roshko, 1988), where ΔU is the velocity difference between the two streams and a the speed of sound. This has been modelled via a number of compressibility corrections, many addressing compressible dissipation and pressure-dilatation, which can both be incorporated in a common two-equation turbulence modelling framework. Most of these models are based on the turbulent Mach number $Ma_t = \sqrt{2k}/a$, with k being the turbulent kinetic energy. Insight gained from recent DNS calculations indicates, however, that such corrections do not reflect the underlying physics well, despite their success for emulating effects of compressibility for selected flow cases. According to DNS studies of turbulent shear layers (Pantano and Sarkar, 2002), the redistribution in the pressure-strain tensor, which becomes less effective with increasing convective Mach number, is responsible for a reduction of levels of turbulence. This appears to be due to the fact that the finite speed of sound and signal propagation yields a decorrelation between pressure and velocity (gradient) fluctuations in the pressure-strain tensor. The gradient Mach number, defined here as $Ma_g = \sqrt{s_{ij}s_{ij}}L/a$, with $s_{ij} = (u_{i,j} + u_{j,i})/2$ and $L = k^{3/2}/\epsilon$, is the ratio of the acoustic time scale to the flow-distortion time scale, and is reported to be the key quantity

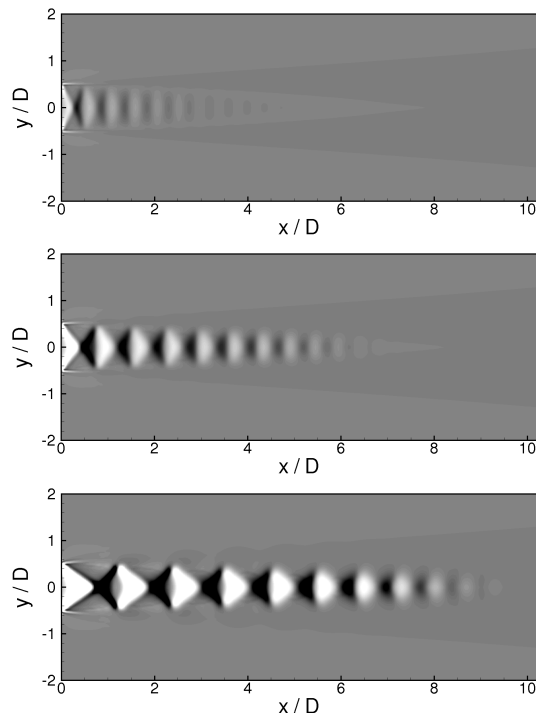


Figure 1: Velocity divergence for turbulent jets with NPR 2.06 (top), 2.32 (middle) and 3.00 (bottom).

in determining the reduction in the pressure-strain tensor for compressible shear flows.

In the special case of the compressible mixing layer, convective, turbulent and gradient Mach numbers can all be directly related to one another, because in self-similar flows all properties will only depend on similarity parameters, and one Mach number is sufficient to describe effects of compressibility (Smits and Dussauge, 2005). Hence, the convective, maximum turbulent and maximum gradient Mach numbers (the last two varying across the layer) only differ by a constant factor, depending on the length scale chosen. However, this is not true for different, more complex types of flows.

Past results from a series of experiments for the compressible mixing layer lead to the "Langley curve", Fig. 2, representing the reduction of spreading with increasing convective Mach number Ma_c , relative to the incompressible levels. Subsequently, several augmentations of existing turbulence models were proposed to account for effects of compressibility, and these were designed to emulate the experimentally observed behaviour.

The majority of the compressibility corrections were developed for two-equation turbulence models and are based on the turbulent Mach number Ma_t (Aupoix, 2000). Most were formulated so as to replicate the effects of compressibility via the explicit pressure-dilatation and/or compressible dissipation. One straightforward addition to the standard $k - \epsilon$ model by Launder and Sharma (1974) is Sarkar's model for the compressible dissipation, i.e. in the form of $\epsilon_d/\epsilon_{inc} = \alpha Ma_t^2$, where α is a coefficient that allows model calibration.

A more elaborate augmentation of a second-moment closure, proposed by El Baz and Launder (1993) and, again, based on the turbulent Mach number, is used here in combination with the TCL second-moment model. The original TCL closure is augmented by additional terms, which are

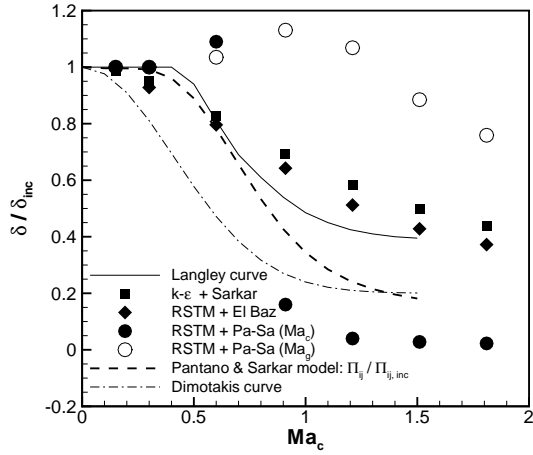


Figure 2: Measured (represented by the "Langley curve") and computed reduction of spreading rate for planar mixing layer due to effects of compressibility on turbulence.

scaled by Ma_t to give

$$\Pi_{ij} = \Pi_{ij,TCL} + 1.5 Ma_t^2 \mathcal{T}_{ij} \quad (1)$$

with Ma_t defined as \sqrt{k}/a in this particular model and \mathcal{T}_{ij} representing additional terms containing velocities, Reynolds stresses and corresponding gradients (details are given by El Baz and Launder (1993)). For the mixing layer, the effects of compressibility are reproduced reasonably well with both approaches, as shown in Fig. 2.

The turbulent- and gradient-Mach-number distributions for the compressible mixing layer with convective Mach number 1.51 are shown in Fig. 3. Each set of three distributions relate to three different streamwise positions. As seen, the two sets are similar. The maximum value for both turbulent and gradient Mach numbers at different streamwise positions remains constant, and the ratio of gradient over turbulent Mach number is about $Ma_g/Ma_t \approx 2.2$.

In the case of an under-expanded jet with NPR 2.32, the gradient Mach number is the only one capable of detecting the shock structure in the jet, as demonstrated in Fig. 4, and models based on the turbulent Mach number, adjusted to reproduce the "Langley curve" well, cannot be expected to do the same for more complex flows. Along the jet centreline, the gradient Mach number is responsive to the shock structure of the jet, while the turbulent Mach number reflects the decay of turbulent kinetic energy from the inflow plane of the domain.

With the suitability of the turbulent Mach number in question, at least for under-expanded jets, attempts have been made to introduce the damping of the components of the pressure-strain tensor proposed by Pantano and Sarkar (2002) for the shear layer as a function of the convective Mach number, modified to depend on a functional relationship for the gradient Mach number. The original model proposed by Pantano and Sarkar is

$$\Pi_{ij}/\Pi_{ij}^I = c + (1-c) \cdot \frac{1 + a Ma_c^2 \exp(-2(2Ma_c - 0.5)^2)}{1 + b Ma_c^2} \quad (2)$$

with Π_{ij}^I as the incompressible pressure-strain tensor and model constants $a = 4.0$, $b = 4.1$ and $c = 0.091$. Pantano and Sarkar report that this model, derived from their DNS of a temporally-developing mixing layer, is compatible with the reduction in spreading rate identified by the dashed line

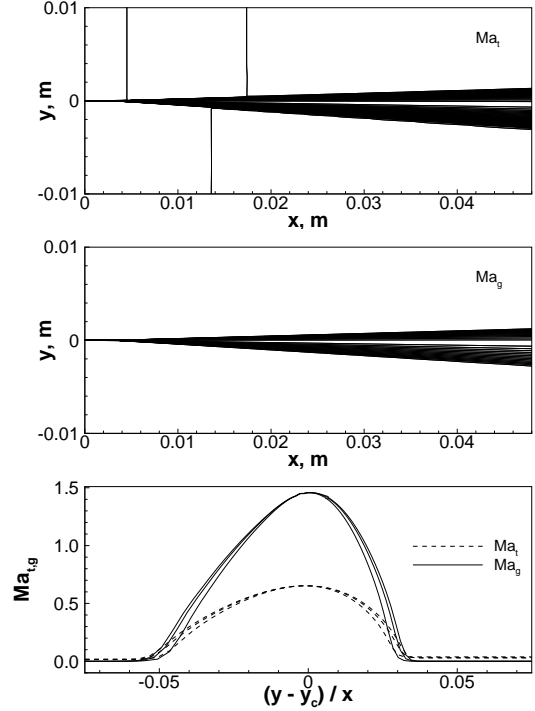


Figure 3: Turbulent (top), gradient (middle) Mach number distribution, and comparison at streamwise positions of $x = 0.02, 0.03$ and $0.04m$ for compressible mixing layer with $Ma_c = 1.51$.

in Fig. 2. The goal in the present work has been to achieve the required reduction of spreading rate in shear layers, but maintain the quality of results obtained for under-expanded jets. However, the damping of pressure-strain tensor components computed with the baseline TCL closure according to Eq. 2 results in an almost sudden shut-down of turbulence in the shear layer above a convective Mach number of 0.6, as illustrated in Fig. 2.

In the mixing layer, the maximum gradient Mach number is found to be close to the convective Mach number, and this has motivated the attempt, with the view to the subsequent use of a variation of Eq. 2 in jets, to replace the latter by the former in Eq. 2. However, without further change, this leads to far too weak a reduction in the spreading rate, as shown in Fig. 2. Indeed, at low values of the convective Mach number, the modification gives an erroneous velocity profile at the edges of the mixing layer, which then results in a slight increase in the spreading rate (defined by the 10% and 90% locations of the velocity difference across the layer).

Fig. 5 shows the budgets for compressible mixing layers at convective Mach numbers $Ma_c = 0.60$ and 1.51 , computed with the reference closure on its own, the reference closure with additional terms for the pressure-strain model, and the reference closure with the components of the pressure-strain model damped uniformly according to suggestions by Pantano and Sarkar for the respective convective Mach number. While the case with the lower convective Mach number produces fairly similar budgets for the modifications of El Baz and Pantano and Sarkar, the latter modification breaks down for the higher convective Mach number, and turbulence essentially collapses. For the shear layer at $Ma_c = 1.51$, the production corresponding to the normal stress obtained in streamwise direction for the reference closure with terms due to the El Baz model matches, and that

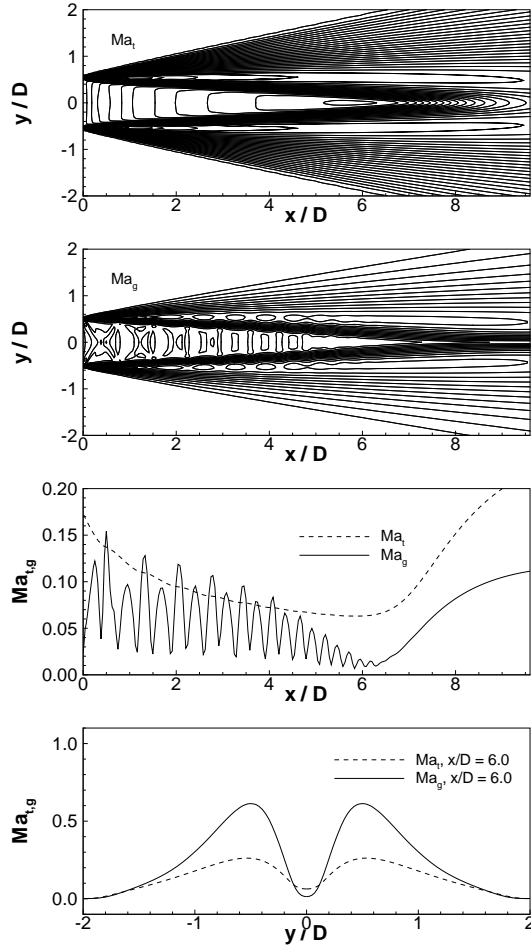


Figure 4: From top to bottom: turbulent and gradient Mach number distributions, behaviour along centre-line and at downstream position of $x/D = 6$ for jet with NPR 2.32.

of shear stress exceeds that of the reference second-moment closure, while the spreading is significantly reduced.

RESULTS FOR JETS

Baseline Turbulence Model

A particular problem posed by the present jets is that the near-field behaviour depends sensitively on the conditions at the nozzle exit. The LDA experiments corresponding to the computations show the exit turbulence intensity to be around 1%, but this level inhibits, with or without the provision of a finite initial shear layer at the jet orifice, the spreading rate and leads to an excessively long potential core. The sensitivity of the potential core to the turbulence intensity is illustrated in Fig. 6 for fully-expanded and in Fig. 7 for under-expanded jets. For the latter case, the decay of the shock-cells is fairly well predicted, but again, this too depends to some extent on the inlet turbulence intensity. Substantial differences between the measurements and the computations arise in respect of the turbulence intensity in the potential core - and this not only because of the difference in the turbulence level at discharge. The computations predict, as expected, a decay in the potential core, while the experiments indicate a rise. However, there are substantial experimental uncertainties in this region, especially at $NPR = 2.32$, which is subjected to rapidly varying

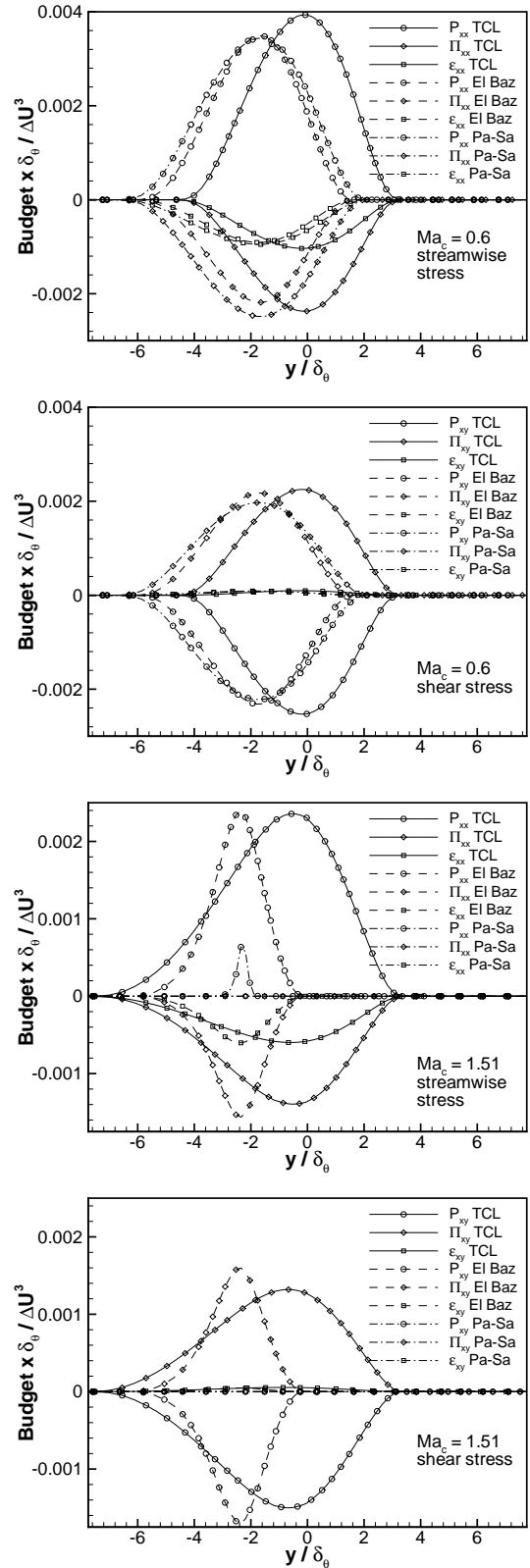


Figure 5: Budgets for shear layer at $Ma_c = 0.60$ and $Ma_c = 1.51$ at $x = 0.04m$. P_{ij} - production, Π_{ij} - redistribution, ϵ_{ij} - dissipation; TCL - reference closure, El Baz - reference closure with El Baz terms, Pa-Sa - reference closure with Pantano and Sarkar damping, based on fixed Ma_c . Normalisation by momentum thickness δ_θ of reference closure (TCL).

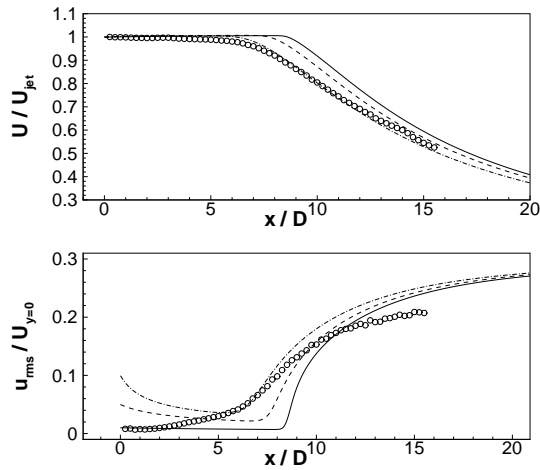


Figure 6: Comparison of centre-line velocity and velocity fluctuation for NPR 1.68 with initial turbulence intensity for jet $Tu = 1\%$ (—), $Tu = 5\%$ (---), $Tu = 10\%$ (- · -), and experimental result (o).

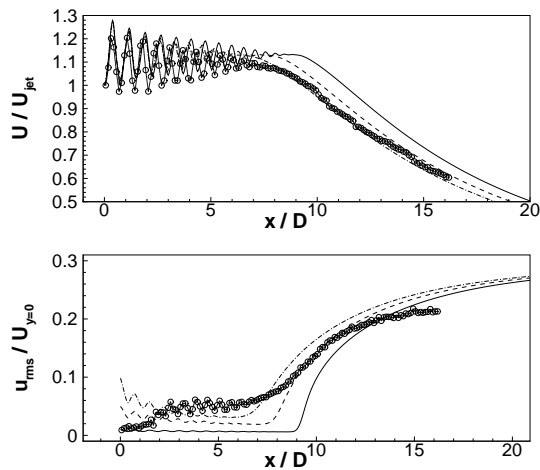


Figure 7: Comparison of centre-line velocity and velocity fluctuation for NPR 2.32 with initial turbulence intensity for jet $Tu = 1\%$ (—), $Tu = 5\%$ (---), $Tu = 10\%$ (- · -), and experimental result (o).

strain and buffeting from the outer region, the latter interpreted by the measurements within the potential core as turbulence. For this case, the predictions show weak local amplification of turbulence due to the oblique shocks, with overall decay. This behaviour can only be achieved with second-moment closure (unless synthetic limiters are embedded in eddy-viscosity models).

Streamwise-normal-stress and shear-stress distributions for a NPR of 2.32 are presented in Figs. 8 and 9, respectively, from which the experimental results are seen to be reproduced computationally with excellent accuracy. A similar quality of agreement is also observed for the radial normal stress, not included herein. The only discrepancy relates to the normal stress in the region of the potential core, reflecting both the experimental and computational difficulties discussed earlier.

Compressibility Corrections

The present results indicate that, for the range of nozzle-pressure ratios considered, corrections due to effects of com-

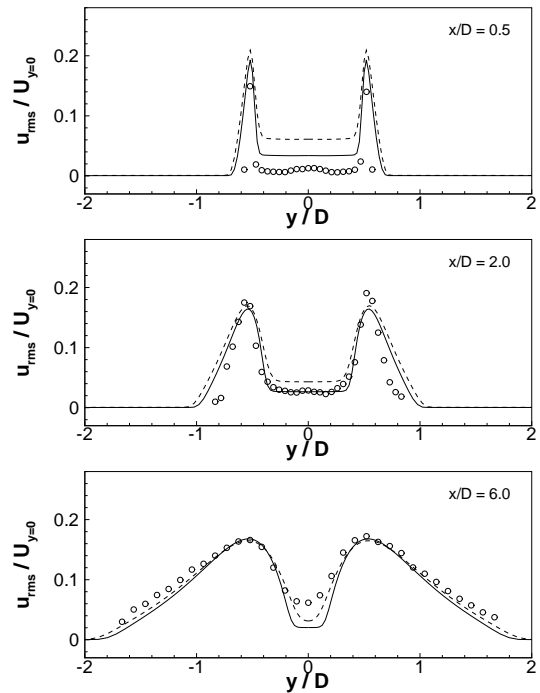


Figure 8: Comparison of normal stresses for NPR 2.32 at selected streamwise positions with initial turbulence intensity for jet $Tu = 5\%$ (—), $Tu = 10\%$ (---), and experimental result (o).

pressibility are not appropriate or useful. The convective Mach number derived from the maximum velocity obtained for a jet at NPR 2.32 and the corresponding sound speed does not exceed 0.61, a region where effects of compressibility in shear layers are weak. Computations with the same turbulence model, including modifications to the pressure-strain model to account for effects of compressibility in shear layers, produced less accurate results, as illustrated in Fig. 10. The profiles of velocity and Reynolds stresses also show corresponding (mild) deteriorations.

CONCLUSIONS

Compressible fully- and under-expanded jets were computed for NPRs up to 3, employing a sophisticated second-moment closure, and compared with results from corresponding LDA measurements. Apart from the nozzle-near field, the baseline turbulence model predicted the normal and shear stresses in the jet with good accuracy.

Compressibility corrections, designed to replicate the response of compressible mixing layers to the convective Mach number, are found to worsen the agreement with the experimental results for the compressible jets, although the quantitative change in the predicted results is minor, reflecting the fact that the maximum mixing-layer-equivalent values for the convective Mach number in the present jets are low, of order 0.6 or below. The Pantano-Sarkar model for the compressibility-attenuated pressure-strain process performs poorly in conjunction with the particular second-moment closure used herein, failing to replicate the "Langley curve" and causing a collapse of the turbulence activity beyond a convective Mach number of 0.8. Thus, further work is needed.

For future work, the consideration of jets with higher NPR, containing Mach disks, would be of particular interest

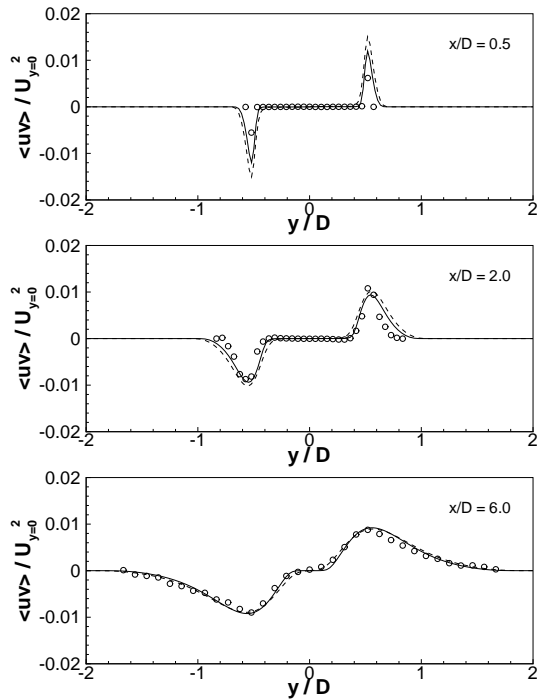


Figure 9: Comparison of shear stresses for NPR 2.32 at selected streamwise positions with initial turbulence intensity for jet $Tu = 5\%$ (—), $Tu = 10\%$ (---), and experimental result (\circ).

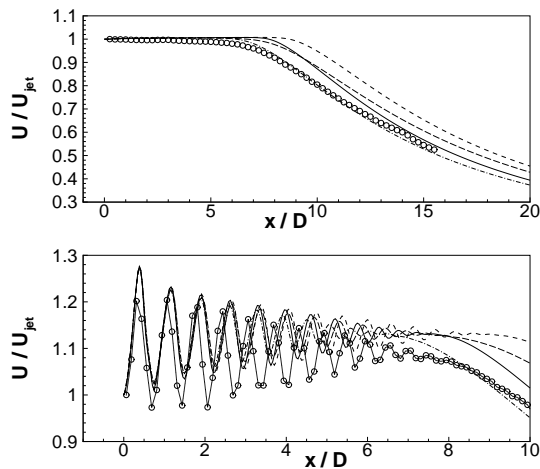


Figure 10: Comparison of centre-line velocity for compressibility model corrections (El Baz and Launder) for NPR 1.68 (top) and 2.32 (bottom), with initial turbulence intensity for jet $Tu = 5\%$ (—), the same with El Baz additions (---), $Tu = 10\%$ (- · -), the same with El Baz additions (— · —), and experimental result (\circ).

to further investigate the shock-turbulence interaction.

ACKNOWLEDGEMENTS

The financial support of EPSRC and BAE Systems is gratefully acknowledged. Further, the authors would like to thank P. Batten and T. Craft for their assistance and contributions during the course of the project.

REFERENCES

Anderson, N., "A study of Mach 0.75 Jets and Their

Radiated Sound Using Large-Eddy Simulation", Division of Thermo and Fluid Dynamics, Chalmers University of Technology, 2003

Aupoix, B., "Introduction to Turbulence Modelling for Compressible Flows", von Karman Lecture Series, 2000

Batten, P., Craft, T. J., Leschziner, M. A. and Loyau, H., "Reynolds-Stress-Transport Modeling for Compressible Aerodynamics Applications", AIAA Journal, 37(7):785–796

Batten, P., Leschziner, M. A. and Goldberg, U.C., "Average-State Jacobians and Implicit Methods for Compressible Viscous and Turbulent Flows", JCP, 137:38–78, 1997

Berland, J., Bogey, C. and Bailly, C., "Large Eddy Simulation of Screech Tone Generation in a Planar Under-expanded Jet" AIAA-2006-2496, 12th AIAA/CEAS Aeroacoustics Conference, Cambridge, Massachusetts, 2006

Bodony, D., Ryu, J., Ray P. and Lele S., "Investigating Broadband Shock-Associated Noise of Axisymmetric Jets Using Large-Eddy Simulation", AIAA-2006-2495, 12th AIAA/CEAS Aeroacoustics Conference, Cambridge, Massachusetts, 2006

Craft, T. J. and Launder, B. E., "A Reynolds stress closure designed for complex geometries", Int. J. Heat and Fluid Flow, 17:245–254, 1996

Dash, S. M., Wolf, D. E. and Seiner, J. M., "Analysis of Turbulent Underexpanded Jets, Part I: Parabolized Navier-Stokes Model, SCIPVIS", AIAA Journal, 23(4):505–514, 1985

El Baz, A. M. and Launder, B. E., "Second-Moment Modelling of Compressible Mixing Layers", Engineering Turbulence Modelling and Experiments 2, Editors: Rodi and Martelli, Elsevier, 63–72, 1993

Feng, T. and McQuirk, J., "LDA Velocity Measurements of Fully- and Under-Expanded Nozzle Flows", private communication, 2005

Launder, B. E. and Sharma, B. I., "Application of the energy-dissipation model of turbulence to the calculation of flow near a spinning disk", Letters of Heat and Mass Transfer, 1:131–138, 1974

Leschziner, M. A., Batten, P. and Craft, T. J., "Reynolds-stress modelling of transonic afterbody flows", The Aeronautical Journal, Royal Aeronautical Society, 297–306, June 2001

Pantano, C. and Sarkar, S., "A study of compressibility effects in the high-speed turbulent shear layer using direct simulation", Journal of Fluid Mechanics, 451:329–371, 2002

Pao, S. P. and Abdol-Hamid, K. S., "Numerical Simulation of Jet Aerodynamics Using the Three-Dimensional Navier-Stokes Code PAB3D", NASA TP 3596, 1996

Papamoschou, D. and Roshko, A., "The compressible turbulent shear layer: an experimental study", Journal of Fluid Mechanics, 197:453–477, 1988

Seiner, J. M., Dash, S. M. and Wolf, D. E., "Analysis of turbulent underexpanded jets, Part II: Shock Noise Features Using SCIPVIS", AIAA Journal, 23(5):669–677, 1985

Smits, A. J. and Dussauge, J.-P., "Turbulent Shear Layers in Supersonic Flow", Springer, 2005

Viswanathan, K., Shur, M., Strelets, M. and Spalart, P. R. "Numerical Predictions from Round and Beveled Nozzles", Euromech Colloquium 467: Turbulent Flow and Noise Generation, Marseille, 2005

Vreman, A. W., Sandham, N. D. and Luo, K. H., "Compressible mixing layer growth rate and turbulence characteristics", Journal of Fluid Mechanics, 320:235–258, 1996